Atmospheric Environment 86 (2014) 120–128

Contents lists available at ScienceDirect

Atmospheric Environment

journal homepage: www.elsevier.com/locate/atmosenv

Diurnal variation of NO_x and ozone exchange between a street canyon and the overlying air

Kyung-Hwan Kwak, Jong-Jin Baik*

School of Earth and Environmental Sciences, Seoul National University, Seoul 151-742, Republic of Korea

HIGHLIGHTS

- The diurnal variation of NO_x and O_3 exchange in a street canyon is numerically investigated.
- Differential wall heating is important for determining NO_x and O_3 exchange.
- The exchange by mean flow can be comparable to that by turbulent flow in the afternoon.
- NO_x and O_3 exchange velocities are individually estimated.
- The exchange velocity depends on photochemistry as well as flow in the street canyon.

ARTICLE INFO

Article history:
Received 16 May 2013
Received in revised form
14 October 2013
Accepted 19 December 2013

Keywords:
Street canyon
NO_x removal
O_3 entrainment
Diurnal variation
Surface heating
CFD model

ABSTRACT

The diurnal variation of NO_x and O_3 exchange between a street canyon and the overlying air in two dimensions is investigated to understand reactive pollutant removal and entrainment across the roof level of the street canyon. The computational fluid dynamics (CFD) model used in this study is a Reynolds-averaged Navier–Stokes equations (RANS) model and includes the urban surface and radiation processes and the comprehensive chemical processes. The CFD model is used for the one-day simulation in which the easterly ambient wind blows perpendicular to the north–south oriented street canyon with a canyon aspect ratio of 1. In the morning when the surface temperature of the downwind building wall is higher than that of the upwind building wall, two counter-rotating vortices appear in the street canyon (flow regime II). In the afternoon when the surface temperature of the upwind building wall is higher than that of the downwind building wall, an intensified primary vortex appears in the street canyon (flow regime I). The NO_x and O_3 exchange is generally active in the region close to the building wall with the higher temperature regardless of flow regime. The NO_x and O_3 exchange by turbulent flow is dominant in flow regime II, whereas the NO_x and O_3 exchange by mean flow becomes comparable to that by turbulent flow in a certain period of flow regime I. The NO_x and O_3 exchange velocities are similar to each other in the early morning, whereas these are significantly different from each other around noon and in the afternoon. This behavior indicates that the exchange velocity is dependent on flow regime. In addition, the diurnal variability of O_3 exchange velocity is found to be dependent on photochemistry rather than dry deposition in the street canyon. This study suggests that photochemistry as well as flow in a street canyon is needed to be taken into account when exchange velocities for reactive pollutants are estimated.

1. Introduction

Poor air quality in street canyons is a severe problem as people are directly exposed to the polluted air that is not easily ventilated out but remains in the proximity of mobile sources. As a way of improving air quality in street canyons, pollutant removal as well as emission control has been an interesting issue in numerous studies that cover dispersion, chemical transformation, and deposition processes (Vardoulakis et al., 2003).

Pollutant dispersion in a street canyon is closely associated with flow therein, which is dependent on the canyon aspect ratio (Lee and Park, 1994; Barlow et al., 2004; Cai et al., 2008; Chung and Liu, 2013) and surface heating intensity (Sini et al., 1996; Baik and Kim, 1999; Xie et al., 2007; Li et al., 2012). These previous studies have shown that pollutant removal from a street canyon becomes efficient as the canyon aspect ratio decreases or the surface heating

* Corresponding author. Tel.: +82 2 880 6990; fax: +82 2 883 4972.
E-mail address: jjbaik@snu.ac.kr (J.-J. Baik).

1352-2310/$ – see front matter © 2013 Elsevier Ltd. All rights reserved.
http://dx.doi.org/10.1016/j.atmosenv.2013.12.029

intensifies. In an isothermal condition, pollutant removal across the roof level of the street canyon where the wind shear is large is mostly dominated by turbulent flow rather than by mean flow (Baik and Kim, 2002; Liu and Barth, 2002). However, pollutant removal by mean flow can be comparable to that by turbulent flow when the surface (road or upwind building-wall) heating (Kang et al., 2008; Tay et al., 2010) or the building-roof cooling (Baik et al., 2012) enhances flow in a street canyon. When the downwind building wall is heated, the contribution of mean flow to pollutant removal can be small or considerable depending on surface heating intensity (Cai, 2012; Park et al., 2012).

Gaseous pollutants in street canyons are not passive but reactive, for which chemical transformation and deposition are important processes. Simple photochemistry between NO, NO_2, and O_3 was coupled with computational fluid dynamics (CFD) models to investigate the dispersion of the reactive pollutants in a street canyon (Baker et al., 2004; Baik et al., 2007). A complex chemical mechanism coupled with a CFD model enables us to investigate the dispersion of various reactive pollutants in a street canyon (Kwak and Baik, 2012; Bright et al., 2013). Most recently, Kwak et al. (2013) compared the roles of transport (=advection + turbulent diffusion) and chemical production/loss for several reactive pollutants using the CFD model coupled with a complex chemical mechanism. Previous studies have indicated that the contribution of chemical production/loss to the pollutant concentration can be comparable to that of transport for secondary pollutants (e.g., O_3) rather than primary pollutants.

In the daytime, the variation of incoming solar radiation continuously induces the variation of flow in a street canyon (Offerle et al., 2007). Kwak et al. (2011) performed the one-day simulations of street-canyon flow using a CFD model coupled with the urban surface and radiation processes and classified the street-canyon flow into two flow regimes showing different vortex configurations in the daytime. It is expected that the diurnal variation of flow in a street canyon can cause a substantial variation of reactive pollutant dispersion. Over such a diurnal time scale, the effects of shadow on photochemistry (Grawe et al., 2007) and dry deposition (Pugh et al., 2012) can be important for reactive pollutant dispersion. Kim et al. (2012) implemented complex chemical transformation and dry deposition processes into a CFD model and examined air quality in a street canyon regarding gaseous pollutants and particulate matters. The first aim of this study is to examine the effects of surface heating on the diurnal variations of NO_x removal and O_3 entrainment by considering the effects of shadow on photochemistry and dry deposition. Of many reactive pollutants, NO_x (=NO + NO_2) is emitted near the road in a street canyon and then removed from the street canyon like a passive scalar, whereas O_3 is entrained into a street canyon and then participates in the NO-to-NO_2 conversion. Because of their opposite directions of transport across the roof level, NO_x and O_3 have contrasted transport mechanisms (Kikumoto and Ooka, 2012). In this study, we systematically elucidate the contrasted transport mechanisms of reactive pollutants across the roof level in their diurnal variations.

The efficiency of pollutant removal from a street canyon has been frequently quantified by estimating an exchange velocity or a transfer velocity. The exchange velocity is known to be dependent on the canyon geometry (Barlow and Belcher, 2002; Harman et al., 2004), inflow wind speed (Barlow et al., 2004; Murena et al., 2011), and external turbulence (Caton et al., 2003; Salizzoni et al., 2009). In addition, Cai (2012) recently reported the influences of wall heating on exchange velocity. It is noted that these previous studies have estimated the exchange velocity only for passive scalars released from sources inside a street canyon, assuming that the background concentration is zero. Unlike NO_x that is often regarded as a passive scalar, O_3 is reactive and has a higher concentration in the background than in a street canyon. As an extension of the previous studies, it would be interesting to study exchange velocities for reactive pollutants. The second aim of this study is to compare NO_x and O_3 exchange velocities and examine the dependencies of exchange velocity on flow, photochemistry, and dry deposition in a street canyon.

2. Methods and validation

2.1. CFD model

The CFD model used in this study is a Reynolds-averaged Navier–Stokes equations (RANS) model (Kim and Baik, 2004; Baik et al., 2007) with the renormalization group (RNG) $k-\varepsilon$ turbulence closure scheme, which includes the urban surface and radiation processes (Ryu et al., 2011) and the complex chemical mechanism (carbon bond mechanism IV (CBM-IV); Gery et al., 1989). The coupled CFD model prognostically calculates three mean velocity components, air temperature, turbulent kinetic energy and its dissipation rate, concentrations of reactive species, and surface (i.e., roof, upwind building wall, downwind building wall, and road) temperatures. To integrate the stiff system of photochemical reactions, the Eulerian backward iteration (EBI) method (Hertel et al., 1993) is used. Detailed information on the urban surface and radiation processes and the CBM-IV that are included in the CFD model is given in Kwak et al. (2011) and Kwak and Baik (2012), respectively.

2.2. Vertical transport

The transport equation of a species is expressed as

$$\frac{\partial C_i}{\partial t} + U_j\frac{\partial C_i}{\partial x_j} = D\frac{\partial^2 C_i}{\partial x_j \partial x_j} + \frac{\partial}{\partial x_j}\left(K_c\frac{\partial C_i}{\partial x_j}\right) + \left[\frac{\partial C_i}{\partial t}\right]_{\text{chem}} + \left[\frac{\partial C_i}{\partial t}\right]_{\text{depo}}. \quad (1)$$

Here C_i is the mean concentration of the ith species, U_j is the jth mean velocity component, D is the molecular diffusivity of the species, and K_c is the eddy diffusivity of the species. The last two terms on the right hand side of Eq. (1) are the net chemical production term of the species calculated by the CBM-IV and the dry deposition loss term of the species, respectively. The dry deposition loss term is calculated by

$$\left[\frac{\partial C_i}{\partial t}\right]_{\text{depo}} = -\frac{V_{d,i}}{\Delta}C_i, \quad (2)$$

where $V_{d,i}$ and Δ are the deposition velocity and the distance from the surface, respectively (Pugh et al., 2012). This term is only activated at the grid points nearest to the surfaces.

The vertical mean flux of the ith species ($F_{m,i}$) and the vertical turbulent flux of the ith species ($F_{t,i}$) are calculated using

$$F_{m,i} = C_i W, \quad (3)$$

$$F_{t,i} = \overline{c_i w} = -K_c\frac{\partial C_i}{\partial z}. \quad (4)$$

Here W is the mean vertical velocity, c_i is the deviation from C_i, and w is the deviation from W. The vertical mean and turbulent fluxes are calculated and analyzed for NO_x and O_3 to examine the NO_x removal and O_3 entrainment in a street canyon.

2.3. Exchange velocity

The exchange velocity is defined as the spatially averaged mass exchange between a canyon and the overlying air (Bentham and Britter, 2003; Solazzo and Britter, 2007), which is different from the transfer velocity that reflects the mass transfer from a source at a surface to a canyon or the overlying air (Barlow and Belcher, 2002). The exchange velocity is used as a parameter measuring pollutant exchange between a street canyon and the overlying air. The exchange velocity of the ith species (ω_i) can be calculated using

$$\omega_i = \frac{\langle F_i \rangle}{C_{C,i} - C_{B,i}}, \tag{5}$$

$$\text{where } F_i = F_{m,i} + F_{t,i}. \tag{6}$$

Here F_i is the total vertical flux of the ith species, $C_{C,i}$ is the concentration of the ith species averaged inside the street canyon, and $C_{B,i}$ is the background concentration of the ith species. $\langle\rangle$ denotes the horizontal average at the roof level of the street canyon. The exchange velocity can be rewritten in terms of each flux component by substituting Eq. (6) into Eq. (5):

$$\omega_{m,i} = \frac{\langle F_{m,i} \rangle}{C_{C,i} - C_{B,i}}, \tag{7}$$

$$\omega_{t,i} = \frac{\langle F_{t,i} \rangle}{C_{C,i} - C_{B,i}}. \tag{8}$$

Here $\omega_{m,i}$ and $\omega_{t,i}$ are the mean and turbulent exchange velocities of the ith species, respectively. When the concentration of a species, such as NO_x, is higher in the street canyon than in the background, both the turbulent vertical flux and the concentration difference in Eq. (8) are positive. On the other hand, when the concentration of a species, such as O_3, is higher in the background than in the street canyon, both the turbulent vertical flux and the concentration difference in Eq. (8) are negative. Thus, the turbulent exchange velocity calculated using Eq. (8) is always positive regardless of species.

2.4. Validation

The CFD model has been extensively validated using several wind tunnel experiment and field measurement datasets (Baik et al., 2007, 2012; Kwak et al., 2011; Kwak and Baik, 2012). The series of model validation has consistently confirmed the accuracy of the CFD model coupled with the urban surface and radiation processes and the CBM-IV. An additional validation for transfer velocity is performed against the wind tunnel experiment data of Barlow et al. (2004). In the wind tunnel experiments, transfer velocities with different inflow wind speeds were obtained in street canyons under an isothermal condition using the naphthalene sublimation technique. In the simulations, the emission of passive scalar is modeled using the wall function for scalar described in Cai et al. (2008) when dry deposition process is not considered. Fig. 1 shows the transfer velocities in the street canyon with a canyon aspect ratio of 1 as a function of inflow wind speed when the source of passive scalar is located at the road. The linear relationship between the transfer velocity and the inflow wind speed is reasonably well reproduced by the CFD model. The transfer coefficient (i.e., the transfer velocity normalized by the inflow wind speed) is estimated using the slope of the linear regression with a zero offset in Fig. 1. The transfer coefficient in the simulations (0.00208) is slightly larger than that in the wind tunnel experiments (0.00192), which is acceptable compared to 0.00179 obtained by Cai et al. (2008) and 0.00213 obtained by Cheng and Liu (2011). The deviation in transfer coefficient is to some extent attributed to uncertainties in the representation of emission and/or inflow wind profile.

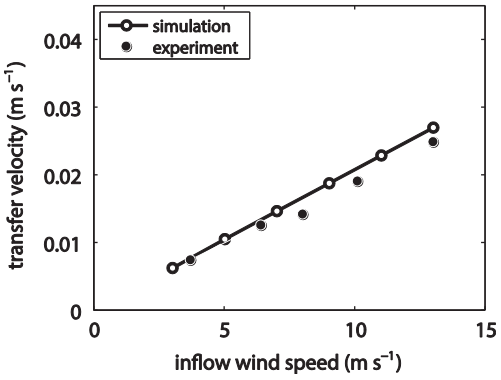

Fig. 1. Transfer velocities estimated in the simulations (open circle) and in the wind tunnel experiments (closed circle) as a function of inflow wind speed.

3. Simulation setup

A two-dimensional (2-D) idealized street canyon is considered (Fig. 2). The building height (H) is 20 m and the street canyon width (W) is 20 m, giving a canyon aspect ratio (H/W) of 1. The grid interval in the x-direction is 0.5 m, and the grid interval in the z-direction is uniformly 0.5 m up to $z = 32$ m and then increases with an expansion ratio of 1.1. The computational domain size is 40 m in the x-direction and 60.1 m in the z-direction. The inflow wind blows in the x-direction, and constant wind speed (=3 m s^{-1}) and turbulent kinetic energy (=0.11 m^2 s^{-2}) are set to be vertically uniform at the inflow boundary to remove the arbitrariness of inflow profiles especially for the estimation of exchange velocity (Solazzo and Britter, 2007). We selected 18 June 2007 (the same day as in Kwak et al. (2011)) in Seoul, Republic of Korea, for estimating the sky radiation. The ambient air temperatures at the inflow

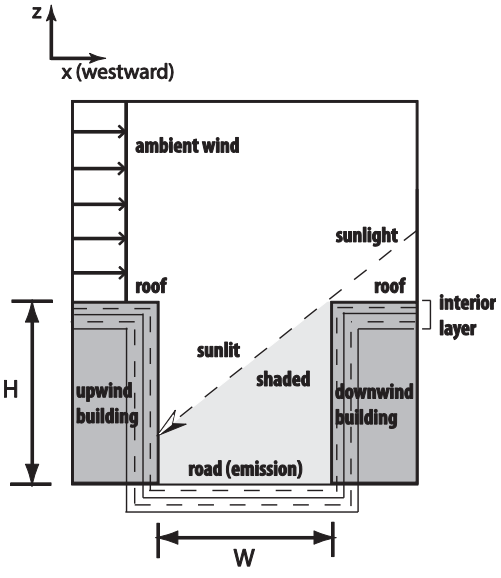

Fig. 2. Illustration of building and street canyon configuration. The street canyon is divided into sunlit and shaded spaces. H is the building height, and W is the street canyon width.

boundary are the same as the observed air temperatures during the day. For a detailed description of the thermal properties of surfaces and substrates, see Kwak et al. (2011). The zero gradient boundary condition is applied at the outflow and upper boundaries.

In this study, the diurnal variations of inflow concentrations and pollutant emission rates as well as inflow wind speed are neglected to isolate the effects of diurnally varying surface heating. The initial and inflow concentrations are 10 ppb for NO, 30 ppb for NO_2, 30 ppb for O_3, 200 ppb for CO, and 41 ppb in total for 7 VOCs that are FORM (formaldehyde), ALD_2 (high molecular weight aldehydes), PAR (paraffin carbon bond), OLE (olefin carbon bond), ETH (ethene), TOL (toluene), and XYL (xylene). NO_x, CO, and the 7 VOCs are emitted at the lowest model level ($z/H = 0.0125$). The emission rate of NO_x is 2 ppb s^{-1} (equivalent to 0.64 μg s^{-1}) per a grid point, the relative portion of NO_x emission rate in the unit of ppb s^{-1} is 9:1 ($NO:NO_2$). The emission rate of the total 7 VOCs is also 2 ppb s^{-1} per a grid point, the relative portions of the 7 VOCs emission rates in the unit of ppb s^{-1} are 56.3% for PAR, 12.4% for TOL, 11.9% for XYL, 9.5% for ETH, 6.7% for OLE, 2.1% for ALD_2, and 1.1% for FORM (Bossioli et al., 2002; Kwak and Baik, 2012). The emission rate of CO is ten times larger than that of NO_x. The model is integrated for 24 h with a dynamics time step of 0.1 s and a chemistry time step of 1 s.

The shading effect on photochemistry is included by separating a canyon space into a sunlit space and a shaded space based on the direct shortwave radiation reaching the surfaces in the street canyon (Fig. 2). The shortwave radiation in a sunlit space consists of direct, diffuse, and reflected radiation, whereas the shortwave radiation in a shaded space consists of diffuse and reflected radiation. Photolysis rate coefficients obtained from Jacobson (2005) are then modified in proportion to the sum of shortwave radiation in each space at every time step.

Dry deposition process is included by calculating deposition fluxes for reactive species at all surfaces. Assuming no vegetation at surfaces, the deposition velocity that is constant over all surfaces is 0.063 cm s^{-1} for NO_2, 0.12 cm s^{-1} for O_3, and 8 cm s^{-1} for HNO_3 (Grøntoft and Raychaudhuri, 2004; Aikawa et al., 2005). The deposition velocity for other reactive species is identically 0.012 cm s^{-1}.

4. Results and discussion

4.1. Surface temperatures and streamline field

The diurnal variations of surface temperatures and streamline field are analyzed and compared with those in the three-dimensional (3-D) simulation of Kwak et al. (2011). Fig. 3 shows the diurnal variations of surface temperatures of roof, upwind building wall, downwind building wall, and road. The surface temperature of the downwind building wall is higher than that of the upwind building wall in the morning (from 0630 to 1230 LST), while the surface temperature of the upwind building wall is higher than that of the downwind building wall in the afternoon (from 1330 LST). The maximum surface temperature (60.8 °C at 1230 LST) appears at the road, and the temperature difference between the road surface and the canyon air is 18.9 °C at the same time. Although the diurnal patterns are quite similar to those in Kwak et al. (2011), the surface temperatures in this study are slightly higher than those in the previous study by up to 4.8 °C (road). This is because the heated air is less mixed with the ambient air in this 2-D simulation than in the 3-D simulation.

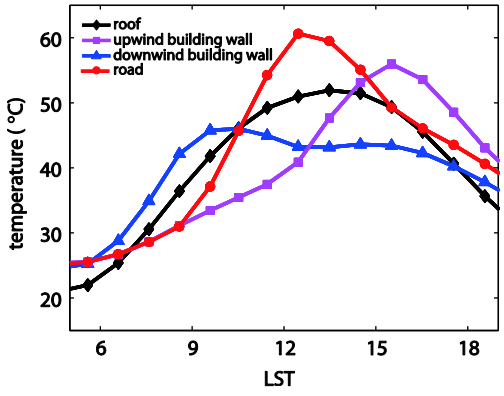

Fig. 3. Diurnal variations of hourly averaged surface temperatures of roof, upwind building wall, downwind building wall, and road.

Fig. 4 shows streamline fields in 2-h intervals from 0500 to 1500 LST. The upper vortex is larger than the lower vortex at 0500, 1300, and 1500 LST, which was classified into flow regime I in the previous study. On the other hand, the lower vortex is larger than the upper vortex at 0900 and 1100 LST, which was classified into flow regime II in the previous study. The transition of flow regime from I to II is captured at 0700 LST, showing three vortices that includes a small vortex with a considerable size near the upwind building wall. Compared to the previous study, the lower vortex tends to be more expanded especially at 0500, 0700, and 1300 LST because the heated air is less mixed with the ambient air in this 2-D simulation. The roof-level-averaged turbulent kinetic energy is obviously higher in flow regime II (e.g., 0.53 m^2 s^{-2} at 1100 LST) than in flow regime I (e.g., 0.16 m^2 s^{-2} at 1500 LST). It is observed that the flow near the roof level where we mainly focus on is similar to that in the previous study. Based on the understanding of the diurnal variation of flow, the diurnal variation of NO_x and O_3 exchange at the roof level is presented and discussed in the next subsection.

4.2. Vertical transport

The vertical transport by mean and turbulent flow at the roof level is the responsible mechanism for pollutant removal from a street canyon and pollutant entrainment into a street canyon. To examine the horizontal and temporal distributions of NO_x transport by mean and turbulent flow, the vertical mean and turbulent NO_x fluxes at the roof level are shown in Fig. 5. In flow regime II, the vertical mean and turbulent NO_x fluxes are the largest at $x/H = 0.4875$ (1030 LST) and $x/H = 0.4625$ (1010 LST), respectively. In flow regime I, a dipole pattern of vertical mean NO_x flux is apparent, and the vertical mean NO_x flux is the largest at $x/H = -0.3875$ (1525 LST). As shown in Fig. 4c and d (flow regime II) and Fig. 4e and f (flow regime I), thermally driven upward flow and thermally intensified upward flow, respectively, are evident along the building wall with the higher temperature, which are important for the vertical NO_x transport in the street canyon. Therefore, it is natural that the vertical mean and turbulent NO_x fluxes are large in the region close to the building wall with the higher temperature. During the transition of flow regime from II to I at about 1240 LST, plenty of poorly ventilated NO_x is removed out of the street canyon because the transition leads to a rapid NO_x mixing in the street canyon. As a result, the vertical turbulent NO_x flux abruptly increases.

In an isothermal condition, the dipole pattern of vertical mean scalar flux at the roof level of the street canyon with a canyon aspect ratio of 1 has been reported (Cai et al., 2008; Li et al., 2009). The vertical turbulent scalar flux exhibits its active region close to the upwind building wall ($x/H \sim -0.2$ in terms of the label in this study) (Liu and Barth, 2002; Liu et al., 2004). When the surface is heated, active regions for scalar transport by both mean and turbulent flow are further shifted toward the upwind building wall

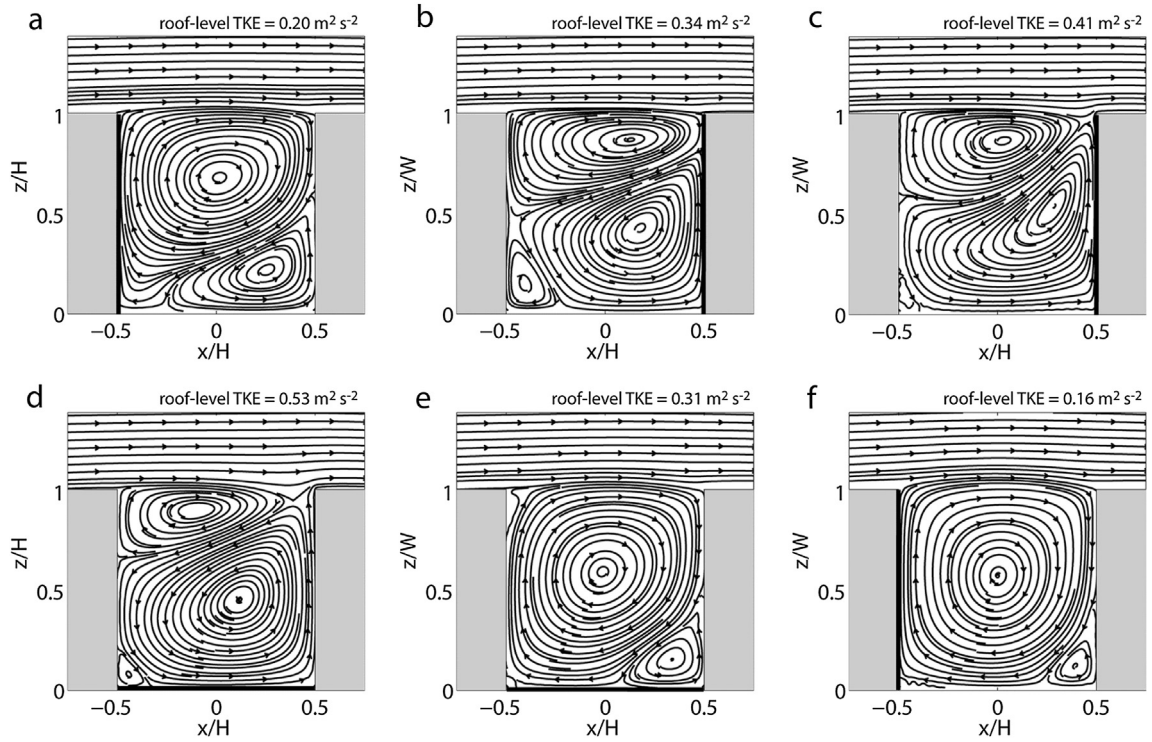

Fig. 4. Streamline fields at (a) 0500, (b) 0700, (c) 0900, (d) 1100, (e) 1300, and (f) 1500 LST. Bold lines indicate the surfaces with the highest temperature. The roof-level-averaged turbulent kinetic energy (TKE) is given on the top of each figure.

(Cheng et al., 2009; Li et al., 2012). The previous studies mentioned above did not consider the effect of dry deposition and the diurnal variation of surface heating. Despite the differences, the features mentioned in the previous studies are qualitatively captured in this study because NO_x, which is conserved during the conversion between NO and NO_2, can be regarded as a passive scalar in a short period of time.

The patterns of the horizontal and temporal distributions of vertical mean and turbulent O_3 fluxes at the roof level (Fig. 6) are similar to those of vertical mean and turbulent NO_x fluxes (Fig. 5).

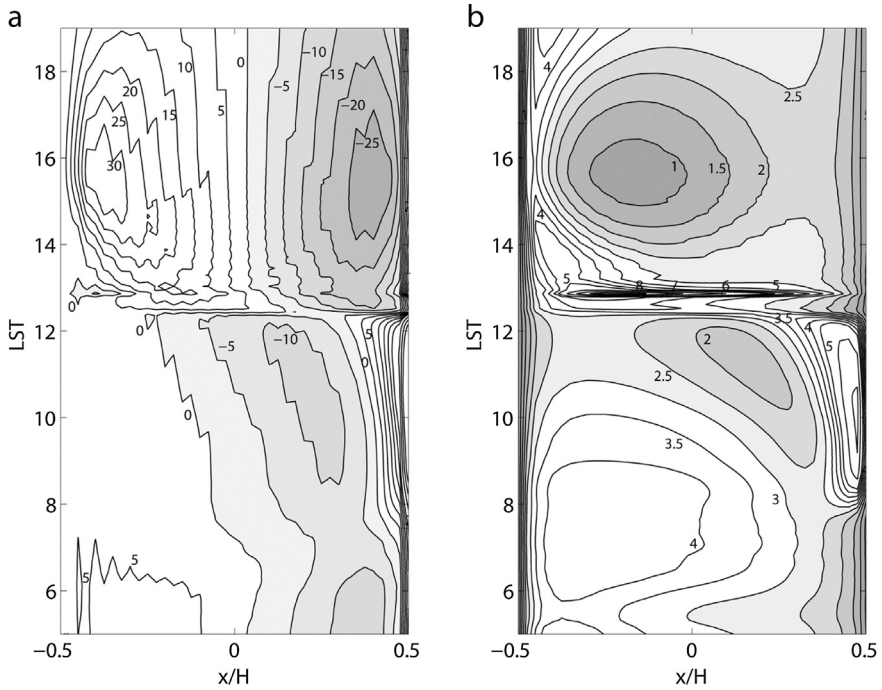

Fig. 5. Diurnal variations of vertical (a) mean and (b) turbulent NO_x fluxes at the roof level. Positive (negative) values denote upward (downward) flux. The unit is ppb m s^{-1}. Shaded areas are for the vertical mean and turbulent NO_x fluxes smaller than 0 and 3 ppb m s^{-1}, respectively.

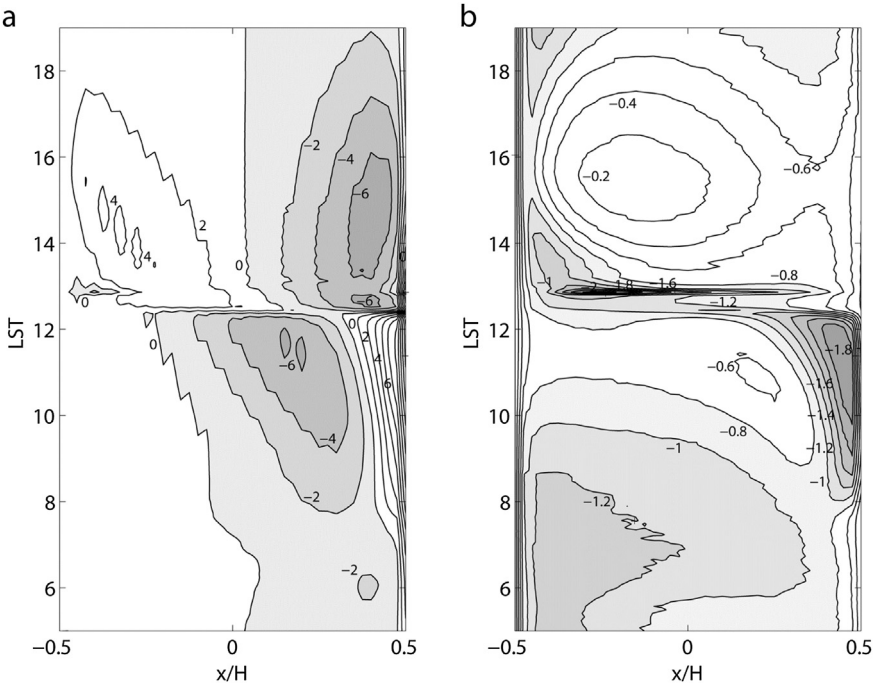

Fig. 6. The same as Fig. 5 but for O_3 fluxes. Shaded areas are for the vertical mean and turbulent O_3 fluxes smaller than 0 and −0.8 ppb m s^{-1}, respectively.

Note that the signs of vertical mean NO_x and O_3 fluxes are the same because these are identically determined by the sign of mean vertical velocity. Unlike the NO_x removal by mean flow, the O_3 entrainment by mean flow is active on the downwind building wall side (but not very close to the wall). In contrast, the signs of vertical turbulent NO_x and O_3 fluxes are opposite to each other because these are individually determined by the signs of vertical NO_x and O_3 concentration gradient, respectively. Accordingly, the NO_x removal and O_3 entrainment by turbulent flow are identically active in the region close to the building wall with the higher temperature.

Fig. 7 shows the diurnal variations of horizontally averaged NO_x and O_3 fluxes at the roof level. It is found that the transport by turbulent flow is mostly responsible for both NO_x removal and O_3 entrainment except for the period of 1430–1530 LST. In flow regime II, the upward mean NO_x flux and downward mean O_3 flux are much smaller than the upward turbulent NO_x flux and downward turbulent O_3 flux, respectively. This can be attributed to the negligible vertical flow at the roof level in relation to the weakened upper vortex as shown in Fig. 4b. After the transition of flow regime from II to I, the upward mean NO_x flux and downward mean O_3 flux evidently increase up to 1.92 ppb m s^{-1} at 1530 LST and 0.43 ppb m s^{-1} at 1430 LST, respectively. For the period of 1430–1530 LST, the contribution of mean flow to the NO_x removal and O_3 entrainment eventually exceeds that of turbulent flow. This can be attributed to the intensified primary vortex expanding over the roof level in flow regime I as shown in Fig. 4f.

The diurnal variation of vertical pollutant flux should be interpreted in association with the diurnal variation of pollutant concentration as well as the diurnal variation of flow. Fig. 8 shows the diurnal variations of canyon-, pedestrian-level- ($z/H = 0.075$), and roof-level-averaged NO_x and O_3 concentrations. The canyon-averaged NO_x concentration is higher in flow regime II than in flow regime I. This agrees with the results of previous studies showing that the scalar concentration in a street canyon is high when two counter-rotating vortices appear in the street canyon in the presence of the downwind building-wall heating (Sini et al., 1996; Kim and Baik, 1999; Xie et al., 2007). The O_3 concentrations are the highest around noon. The differences between the pedestrian-level- and roof-level-averaged concentrations are large in flow regime II with maximum differences of 127 ppb at 0830 LST for NO_x and 17 ppb at 0930 LST for O_3. The large differences in flow regime II are resulted from the weakened vertical NO_x and O_3 transport in the street canyon by the two counter-rotating vortices.

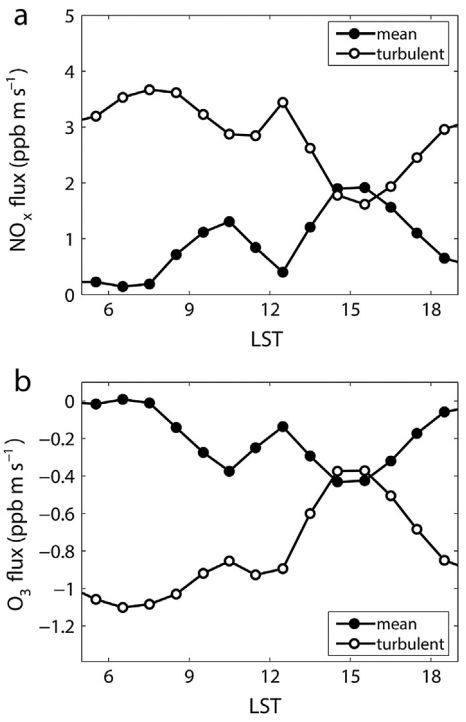

Fig. 7. Diurnal variations of horizontally averaged vertical mean and turbulent (a) NO_x and (b) O_3 fluxes at the roof level. The vertical fluxes are hourly averaged.

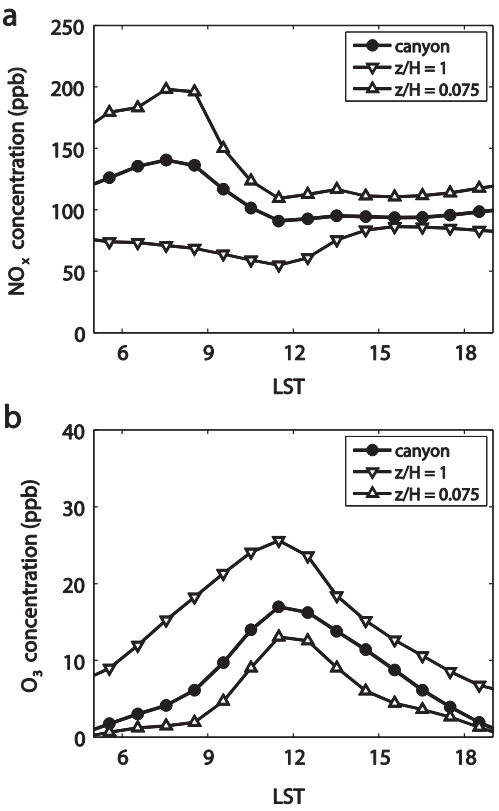

Fig. 8. Diurnal variations of canyon-, pedestrian-level- ($z/H = 0.075$), and roof-level- ($z/H = 1$) averaged (a) NO_x and (b) O_3 concentrations. The concentrations are hourly averaged.

On the contrary, the vertical NO_x and O_3 transport in the street canyon is enhanced by the intensified primary vortex in flow regime I, resulting in the small differences between the pedestrian-level- and roof-level-averaged concentrations.

4.3. Exchange velocity

The efficiencies of NO_x removal and O_3 entrainment are quantified by estimating NO_x and O_3 exchange velocities, respectively, that are individually calculated using Eq. (5). Fig. 9a shows the diurnal variations of NO_x and O_3 exchange velocities. The NO_x and O_3 exchange velocities increase in the morning and then decrease in the afternoon. The NO_x and O_3 exchange velocities are obviously similar to each other only in the early morning. In their mean (Fig. 9b) and turbulent (Fig. 9c) components, the mean NO_x exchange velocity is generally higher in flow regime I than in flow regime II, whereas the turbulent O_3 exchange velocity is lower in flow regime I than in flow regime II. As a result, the O_3 exchange velocity is significantly lower than the NO_x exchange velocity in flow regime I, which in turn emphasizes that the exchange velocities of reactive pollutants depend on flow regime.

Most previous studies adopting an exchange velocity have considered isothermal conditions in which the vertical mean pollutant flux is minor compared to the vertical turbulent pollutant flux at the roof level. Cai (2012) extended the use of exchange velocity in non-isothermal conditions in which the vertical mean pollutant flux is not minor any further. Based on previous studies, we extend the use of exchange velocity for reactive pollutants removed out or entrained into the street canyon and find that the difference between NO_x and O_3 exchange velocities is significantly large in flow regime I when the vertical mean pollutant fluxes at the roof level are not minor.

Another interesting point is that the diurnal variation of O_3 exchange velocity (0.032–0.091 m s^{-1}) is larger than that of NO_x exchange velocity (0.038–0.073 m s^{-1}). To examine the dependencies of exchange velocity on photochemistry and deposition processes in the street canyon, two additional simulations (hereafter, called the sunlit-canyon simulation and the no-deposition simulation) are performed in which the effect of shadow on photochemistry and the effect of dry deposition are neglected in the street canyon, respectively. Fig. 10 shows the diurnal variations of NO_x and O_3 exchange velocities and canyon-averaged NO_x and O_3 concentrations in the control, sunlit-canyon, and no-deposition simulations. The NO_x exchange velocities in the control and sunlit-canyon simulations are nearly overlapped. The NO_x exchange velocity in the no-deposition simulation is slightly higher than that in other simulations. In contrast, the O_3 exchange velocity in the sunlit-canyon simulation is higher than that in other simulations. For example, the O_3 exchange velocity at 1030 LST increases from 0.077 to 0.090 m s^{-1} when the effect of shadow on photochemistry is neglected. On the other hand, the O_3 exchange velocities in the control and no-deposition simulations show negligible differences between them, although the effects of dry deposition on the NO_x and O_3 concentrations are significant (Fig. 10b and d). This comparison indicates that photochemistry in a street canyon is influential for estimating the exchange velocity of a reactive pollutant, whereas dry deposition in a street canyon is not influential as much as photochemistry.

5. Summary and conclusions

The CFD model incorporating the urban surface and radiation processes and the CBM-IV was used to investigate the diurnal variation of NO_x and O_3 exchange between a street canyon and the

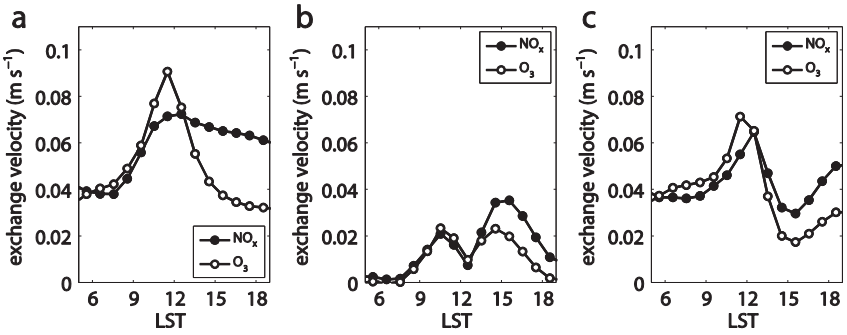

Fig. 9. Diurnal variations of (a) NO_x and O_3 exchange velocities and their (b) mean and (c) turbulent components.

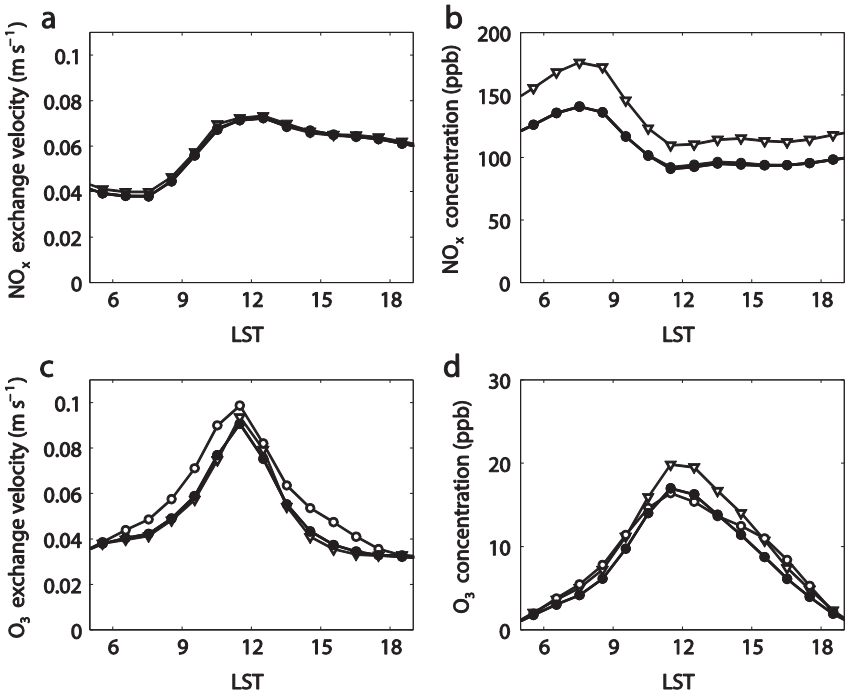

Fig. 10. Diurnal variations of (a) NO_x and (c) O_3 exchange velocities and canyon-averaged (b) NO_x and (d) O_3 concentrations in the control (closed circle), sunlit-canyon (open circle), and no-deposition (open reversed triangle) simulations.

overlying air in two dimensions. As in the previous study, flow regimes I and II are apparent when the surface temperature of the upwind building wall is higher than that of the downwind building wall in the afternoon and the surface temperature of the downwind building wall is higher than that of the upwind building wall in the morning, respectively. The NO_x removal and O_3 entrainment were generally found to be active in the region close to the building wall with the higher temperature. In the diurnal variation, the vertical turbulent NO_x and O_3 fluxes at the roof level are dominant except for the period of 1430–1530 LST when the vertical mean NO_x and O_3 fluxes are larger than the vertical turbulent NO_x and O_3 fluxes, respectively. The partitions of total vertical NO_x and O_3 fluxes into their mean and turbulent components are influenced by the differential wall heating. The two counter-rotating vortices in the morning (flow regime II), which weaken the vertical NO_x and O_3 transport and lead to the large vertical NO_x and O_3 concentration gradients, result in the dominant role of NO_x and O_3 exchange by turbulent flow. On the other hand, the intensified primary vortex in the afternoon (flow regime I), which enhances the vertical NO_x and O_3 transport and lead to the small vertical NO_x and O_3 concentration gradients, results in the comparable role of NO_x and O_3 exchange by mean flow. The NO_x and O_3 exchange velocities were individually estimated. The NO_x and O_3 exchange velocities are similar to each other in the early morning. However, the O_3 exchange velocity is significantly lower than the NO_x exchange velocity around noon and in the afternoon. The larger diurnal variation of O_3 exchange velocity than that of NO_x exchange velocity indicates the dependency of exchange velocity on photochemistry as well as flow in the street canyon. The estimation of exchange velocity for reactive pollutants provides us a basis for quantifying the exchange process regardless of dry deposition process.

In this study, the representation of shadow in a street canyon is rather crude compared to that in some recent thermo-radiative models (e.g., Bouyer et al., 2011). Also, dry deposition velocities applied at surfaces are simply treated. The CFD model used in this study needs to be improved in the representations of shadow and dry deposition. For the purpose of isolating the effects of surface heating on NO_x and O_3 exchange between a street canyon and the overlying air, the emission rates and background concentrations of reactive pollutants as well as the inflow wind speed are constantly specified. In reality, these vary in time and space. Applications of reactive pollutants exchange between street canyons and the overlying air to real situations would be more realistic if CFD-based flow/air quality models coupled with regional scale meteorology/air quality models were used with real emission inventories. Development of such an integrated modeling system and its use in practical problems as well as basic research would be a challenging problem.

Acknowledgments

The authors are grateful to two anonymous reviewers for providing valuable comments on this work. This work was supported by the National Research Foundation of Korea (NRF) grant funded by the Korea Ministry of Education, Science and Technology (MEST) (No. 2012-0005674).

References

Aikawa, M., Hiraki, T., Tamaki, M., 2005. Estimation of the amount of dry deposition in an urban area (Kobe city, Japan) by the inferential method. Environ. Chem. Lett. 3, 62–65.
Baik, J.-J., Kim, J.-J., 1999. A numerical study of flow and pollutant dispersion characteristics in urban street canyons. J. Appl. Meteorol. 38, 1576–1589.
Baik, J.-J., Kim, J.-J., 2002. On the escape of pollutants from urban street canyons. Atmos. Environ. 36, 527–536.
Baik, J.-J., Kang, Y.-S., Kim, J.-J., 2007. Modeling reactive pollutant dispersion in an urban street canyon. Atmos. Environ. 41, 934–949.
Baik, J.-J., Kwak, K.-H., Park, S.-B., Ryu, Y.-H., 2012. Effects of building roof greening on air quality in street canyons. Atmos. Environ. 61, 48–55.
Baker, J., Walker, H.L., Cai, X., 2004. A study of the dispersion and transport of reactive pollutants in and above street canyons – a large eddy simulation. Atmos. Environ. 38, 6883–6892.

Barlow, J.F., Belcher, S.E., 2002. A wind tunnel model for quantifying fluxes in the urban boundary layer. Bound. Layer Meteorol. 104, 131–150.
Barlow, J.F., Harman, I.N., Belcher, S.E., 2004. Scalar fluxes from urban street canyons. Part I: laboratory simulation. Bound. Layer Meteorol. 113, 369–385.
Bentham, T., Britter, R., 2003. Spatially averaged flow within obstacle arrays. Atmos. Environ. 37, 2037–2043.
Bossioli, E., Tombrou, M., Pilinis, C., 2002. Adapting the speciation of the VOCs emission inventory in the greater Athens area. Water Air Soil Pollut. Focus 2, 141–153.
Bouyer, J., Inard, C., Musy, M., 2011. Microclimatic coupling as a solution to improve building energy simulation in an urban context. Energy Build. 43, 1549–1559.
Bright, V.B., Bloss, W.J., Cai, X., 2013. Urban street canyons: coupling dynamics, chemistry and within-canyon chemical processing of emissions. Atmos. Environ. 68, 127–142.
Cai, X., 2012. Effects of differential wall heating in street canyons on dispersion and ventilation characteristics of a passive scalar. Atmos. Environ. 51, 268–277.
Cai, X.-M., Barlow, J.F., Belcher, S.E., 2008. Dispersion and transfer of passive scalars in and above street canyons – large-eddy simulations. Atmos. Environ. 42, 5885–5895.
Caton, F., Britter, R.E., Dalziel, S., 2003. Dispersion mechanisms in a street canyon. Atmos. Environ. 37, 693–702.
Cheng, W.C., Liu, C.-H., 2011. Large-eddy simulation of flow and pollutant transports in and above two-dimensional idealized street canyons. Bound. Layer Meteorol. 139, 411–437.
Cheng, W.C., Liu, C.-.H., Leung, D.Y.C., 2009. On the correlation of air and pollutant exchange for street canyons in combined wind-buoyancy-driven flow. Atmos. Environ. 43, 3682–3690.
Chung, T.N.H., Liu, C.-H., 2013. On the mechanism of air pollutant removal in two-dimensional idealized street canyons: a large-eddy simulation approach. Bound. Layer Meteorol. 148, 241–253.
Gery, M., Witten, G., Killus, J., Dodge, M., 1989. A photochemical kinetics mechanism for urban and regional scale computer modeling. J. Geophys. Res. 94 (D10), 12925–12956.
Grawe, D., Cai, X.-M., Harrison, R.M., 2007. Large eddy simulation of shading effects on NO_2 and O_3 concentrations within an idealized street canyon. Atmos. Environ. 41, 7304–7314.
Grøntoft, T., Raychaudhuri, M.R., 2004. Compilation of tables of surface deposition velocities for O_3, NO_2 and SO_2 to a range of indoor surfaces. Atmos. Environ. 38, 533–544.
Harman, I.N., Barlow, J.F., Belcher, S.E., 2004. Scalar fluxes from urban street canyons. Part II: model. Bound. Layer Meteorol. 113, 387–409.
Hertel, O., Berkowicz, R., Christensen, J., 1993. Test of two numerical schemes for use in atmospheric transport-chemistry models. Atmos. Environ. 27A, 2591–2611.
Jacobson, M.Z., 2005. Fundamentals of Atmospheric Modeling, second ed. Cambridge, p. 813.
Kang, Y.-S., Baik, J.-J., Kim, J.-J., 2008. Further studies of flow and reactive pollutant dispersion in a street canyon with bottom heating. Atmos. Environ. 42, 4964–4975.
Kikumoto, H., Ooka, R., 2012. A numerical study of air pollutant dispersion with bimolecular chemical reactions in an urban street canyon using large-eddy simulation. Atmos. Environ. 54, 456–464.
Kim, J.-J., Baik, J.-J., 1999. A numerical study of thermal effects on flow and pollutant dispersion in urban street canyons. J. Appl. Meteorol. 38, 1249–1261.
Kim, J.-J., Baik, J.-J., 2004. A numerical study of the effects of ambient wind direction on flow and dispersion in urban street canyons using the RNG k–ε turbulence model. Atmos. Environ. 38, 3039–3048.
Kim, M.J., Park, R.J., Kim, J.-J., 2012. Urban air quality modeling with full O_3–NO_x–VOC chemistry: implications for O_3 and PM air quality in a street canyon. Atmos. Environ. 47, 330–340.
Kwak, K.-H., Baik, J.-J., 2012. A CFD modeling study of the impacts of NO_x and VOC emissions on reactive pollutant dispersion in and above a street canyon. Atmos. Environ. 46, 71–80.
Kwak, K.-H., Baik, J.-J., Lee, S.-H., Ryu, Y.-H., 2011. Computational fluid dynamics modelling of the diurnal variation of flow in a street canyon. Bound. Layer Meteorol. 141, 77–92.
Kwak, K.-H., Baik, J.-J., Lee, K.-Y., 2013. Dispersion and photochemical evolution of reactive pollutants in street canyons. Atmos. Environ. 70, 98–107.
Lee, I.Y., Park, H.M., 1994. Parameterization of the pollutant transport and dispersion in urban street canyons. Atmos. Environ. 28, 2343–2349.
Li, X.-X., Liu, C.-H., Leung, D.Y.C., 2009. Numerical investigation of pollutant transport characteristics inside deep urban street canyons. Atmos. Environ. 43, 2410–2418.
Li, X.-X., Britter, R.E., Norford, L.K., Koh, T.-Y., Entekhabi, D., 2012. Flow and pollutant transport in urban street canyons of different aspect ratios with ground heating: large-eddy simulation. Bound. Layer Meteorol. 142, 289–304.
Liu, C.-H., Barth, M.C., 2002. Large-eddy simulation of flow and scalar transport in a modeled street canyon. J. Appl. Meteorol. 41, 660–673.
Liu, C.-H., Barth, M.C., Leung, D.Y.C., 2004. Large-eddy simulation of flow and pollutant transport in street canyons of different building-height-to-street-width ratios. J. Appl. Meteorol. 43, 1410–1424.
Murena, F., Di Benedetto, A., D'Onofrio, M., Vitiello, G., 2011. Mass transfer velocity and momentum vertical exchange in simulated deep street canyons. Bound. Layer Meteorol. 140, 125–142.
Offerle, B., Eliasson, I., Grimmond, C.S.B., Holmer, B., 2007. Surface heating in relation to air temperature, wind and turbulence in an urban street canyon. Bound. Layer Meteorol. 122, 273–292.
Park, S.-B., Baik, J.-J., Raasch, S., Letzel, M.O., 2012. A large-eddy simulation study of thermal effects on turbulent flow and dispersion in and above a street canyon. J. Appl. Meteorol. Climatol. 51, 829–841.
Pugh, T.A.M., MacKenzie, A.R., Whyatt, J.D., Hewitt, C.N., 2012. Effectiveness of green infrastructure for improvement of air quality in urban street canyons. Environ. Sci. Technol. 46, 7692–7699.
Ryu, Y.-H., Baik, J.-J., Lee, S.-H., 2011. A new single-layer urban canopy model for use in mesoscale atmospheric models. J. Appl. Meteorol. Climatol. 50, 1773–1794.
Salizzoni, P., Soulhac, L., Mejean, P., 2009. Street canyon ventilation and atmospheric turbulence. Atmos. Environ. 43, 5056–5067.
Sini, J.-F., Anquetin, S., Mestayer, P.G., 1996. Pollutant dispersion and thermal effects in urban street canyons. Atmos. Environ. 30, 2659–2677.
Solazzo, E., Britter, R.E., 2007. Transfer processes in a simulated urban street canyon. Bound. Layer Meteorol. 124, 43–60.
Tay, B.K., McFiggans, G.B., Jones, D.P., Gallagher, M.W., Martin, C., Watkins, P., Harrison, R.M., 2010. Linking urban aerosol fluxes in street canyons to larger scale emissions. Atmos. Chem. Phys. 10, 2475–2490.
Vardoulakis, S., Fisher, B.E.A., Pericleous, K., Gonzalez-Flesca, N., 2003. Modelling air quality in street canyons: a review. Atmos. Environ. 37, 155–182.
Xie, X., Liu, C.-H., Leung, D.Y.C., 2007. Impact of building facades and ground heating on wind flow and pollutant transport in street canyons. Atmos. Environ. 41, 9030–9049.